Climate Change Impacts on Flood-induced Industrial Building Losses in a Coastal City of Australia

Hao Qin
Research Fellow, School of Civil and Environmental Engineering, University of Technology Sydney, Sydney, Australia

Mark G. Stewart
Distinguished Professor, School of Civil and Environmental Engineering, University of Technology Sydney, Sydney, Australia

ABSTRACT: Buildings in coastal cities of Australia, mostly located in estuarine and deltaic plains, are vulnerable to various types of floods. The adverse effects of flooding could be further exacerbated with global warming and sea level rise. Steel portal framed industrial buildings are widely used as warehouses, supermarkets, manufacturing workshops and storage facilities, which make up a large portion of the building stock in a city. This paper presents a case study to assess building losses for an industrial area exposed to flood hazards and climate change risks in the City of Mackay, Australia. The flood inundation risks for the study area under current and future climates were obtained from data produced by previous flood studies. Various flood types including riverine (fluvial), overland flow (pluvial) and coastal (storm tide) floods were considered for industrial buildings in the study area. A high-fidelity physics-based vulnerability model was developed for a prototype steel portal frame industrial building considering major damage mechanisms for building components under flood-induced hydrostatic and hydrodynamic loads. Industrial building losses were evaluated based on the vulnerability model and the predicted extreme flood inundation at individual building levels for different average recurrent intervals considering the climate change impacts. The results suggest that the climate change impacts on aggregated building losses for 100-year floods are marginal. For 500-year floods in future climate (year 2100), the aggregated building losses could potentially increase by about 47% for riverine flood and about 176% for coastal flood, whereas the climate change impacts on building losses due to overland flow flood are negligible.

Buildings in coastal cities of Australia, mostly located in estuarine and deltaic plains, are vulnerable to various types of floods (pluvial, fluvial and coastal floods). The adverse effects of flooding could be further exacerbated given the climate change impacts on precipitation, storm intensity and mean sea level. For example, the Australian guide to flood estimation (Ball et al. 2019) recommends applying a climate change factor to increase the precipitation by 2090 and a 20% increase of rainfall depth is provided for many locations in Australia. There is a need to understand flood hazards from various sources in a future climate and their consequent effects on the built environment in coastal communities.

Steel portal framed industrial buildings are widely used as warehouses, supermarkets, manufacturing workshops and storage facilities, which make up a large portion of the building stock in a city. There is currently a lack of high-fidelity physics-based models enabling the vulnerability and risk assessments for this type of buildings exposed to flood loading. Such physics-based vulnerability models facilitate a transparent building risk assessment with explicit physical damage mechanisms that can better capture the impacts of flood and climate hazards on building

losses. It will also support subsequent flood risk management tasks such as cost-benefit analysis and decision support for risk reduction, climate adaptation and resilience enhancement at the building level.

This paper presents a case study to assess building losses for an industrial area exposed to flood and climate change risks in the City of Mackay, Australia. The flood inundation risks for the study area under current and future climates are obtained from data produced by previous flood studies (BMT WBM 2013, WRM 2021a, WRM 2021b) for Mackay. Various flood types including riverine (fluvial), overland flow (pluvial) and coastal (storm tide) floods are considered for industrial buildings in the study area. A high-fidelity physics-based vulnerability model is developed for a prototype steel portal frame industrial building considering major damage mechanisms under flood-induced hydrostatic and hydrodynamic loads. Industrial building losses are then evaluated based on the vulnerability model and the predicted extreme flood inundation at the individual building level for different average recurrent intervals (ARI) considering the climate change impacts.

1. STUDY AREA

The City of Mackay in Central Queensland of Australia is selected in this study, and an industrial area (see Fig. 1) consisting of a number of industrial buildings is of interest for the assessment of flood-induced building losses. The industrial area is located at the northeast of the city on the south shore of the Pioneer River. The sources of floods in this area include riverine flood from the Pioneer River and a few creeks (e.g., Shellgrit Creek and Sandfly Creek), overland flow or pluvial flood due to excessive rainfall and storm tide (storm surge plus astronomical tide) induced by tropical cyclones or other severe storms.

Figure 1: Study area.

2. FLOOD HAZARDS AND CLIMATE CHANGE IMPACTS

2.1. Current climate

The spatially distributed flood inundation levels corresponding to different ARIs for the city of Mackay were obtained from relevant flood studies (BMT WBM 2013, WRM 2021a, WRM 2021b). The inundation levels were determined separately for each type of flood including riverine (fluvial), overland flow (pluvial) and coastal floods, though the compound flood actions were somewhat addressed considering the coincidence of fluvial flooding and storm tide levels (WRM 2021b). The flood models considered the effects of flood defenses (e.g., seawalls, levees) and drainage systems (e.g., water pipes, outlets). The topography and floodplain roughness were characterized by the digital elevation model (DEM) and Manning's 'n' values with information about vegetation types and land uses.

The modelling of riverine and overland flow floods considered interactions between Sandfly and Shellgrit creek catchments, Pioneer River overflows and storm tide (WRM 2021a; WRM 2021b). Two-dimensional rain-on-grid hydraulic and hydrodynamic models were employed to derive the flood inundation mapping for the city floodplains considering different ARIs. Figure 2 shows the Mackay City inundation mapping (WRM 2021a) for riverine flood under the current

climate with a 100-year ARI and a 500-year ARI. The flood inundation from extreme storm tide induced by tropical cyclones and other severe storms were studied by BMT WBM (2013). The extreme storm tide levels (storm surge plus astronomical tide) along the coastline of Mackay induced by tropical cyclones were obtained by Monte Carlo simulations that integrate a stochastic cyclone wind field model and a 2-D hydrodynamic model driven by wind pressures. The effects of the ocean bathymetry and the Great Barrier Reef were considered. The extreme storm tide levels for non-cyclonic storms were obtained by extreme value analysis based on tidal gauge data. The flood inundation mapping from storm tide was then derived using a 'bathtub' approach based on the extreme storm tide levels along the coastline. Wave runup was found to only affect areas very close to shoreline, and hence ignored for coastal flood inundation.

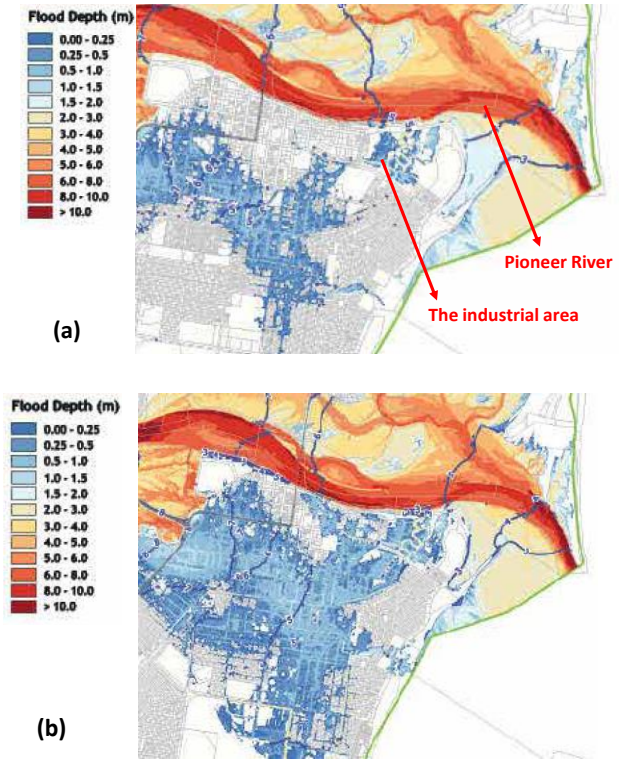

Figure 2: Riverine flood inundation mapping (WRM2021a) for the current climate, (a) 100-year ARI, and (b) 500-year ARI.

2.2. Future climate

According to the guidelines by Queensland government (QLD GOV 2011), a 20% increase in rainfall and a 0.8 m rise in mean sea level by the year of 2100 based on a high greenhouse gas emissions pathway (RCP 8.5) are considered here. The rainfall increase is based on a projected temperature rise of 4° Celsius by 2100. A 10% increase of storm intensity is projected by 2100, however, such increase was found to have a marginal effect on extreme coastal flooding in Mackay (BMT WBM 2013), and hence the climate change impacts on storm intensity are not considered. Figure 3 shows the Mackay City inundation mapping (WRM 2021a) for riverine flood by 2100 considering the climate change impacts with a 100-year ARI and a 500-year ARI. It is observed that, for a given ARI, more areas are inundated under unabated (RCP 8.5) climate change and the inundation depths generally increase when compared with Fig. 2.

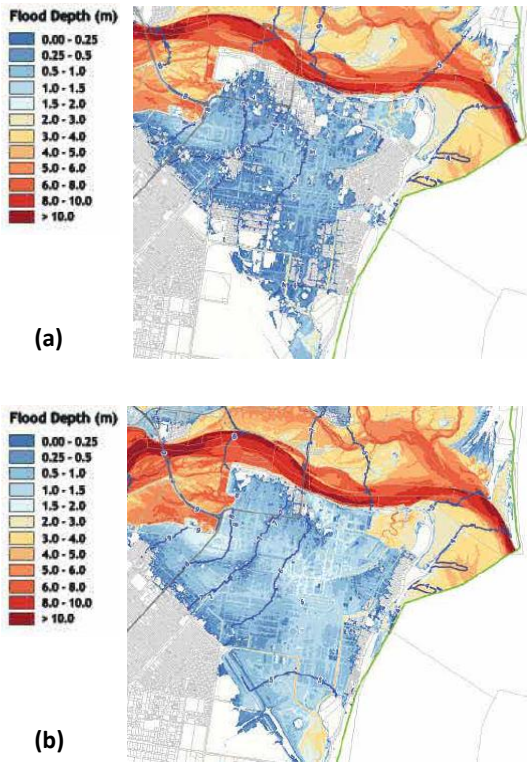

Figure 3: Riverine flood inundation mapping (WRM2021a) for the future climate (2100), (a) 100-year ARI, and (b) 500-year ARI.

3. BUILDING VULNERABILITY

3.1. Vulnerability modelling

In this study, a physics-based vulnerability model was developed for a prototype industrial building as shown in Fig. 4. The steel portal frame industrial building is metal-clad with end wall bracing systems shown in Fig. 4. Fenestrations include windows, personnel doors and overhead roller doors. The prototype industrial building was designed according to relevant Australian design standards considering dead load, live load, wind load and relevant load combinations.

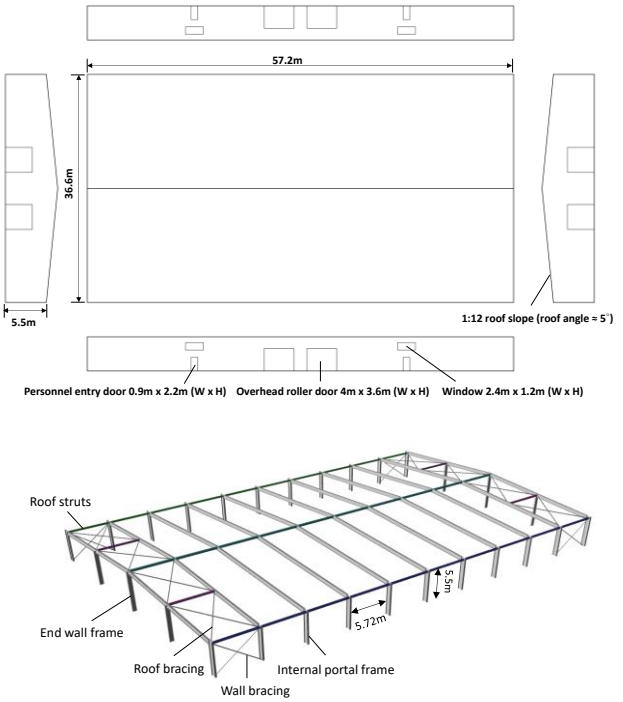

Figure 4: Plan view, steel framing and bracing of the prototype industrial building.

The vulnerability assessment was conducted using an assembly-based approach (e.g., FEMA 2014) by integrating monetary losses derived based on the physical damages of different building subassemblies under flood loads. In this study, building vulnerability is expressed as the expected building loss ratio (ratio of the damage repair or replacement cost to the building value) conditional on relevant flood intensity measures *IM* (i.e., inundation depth and flow velocity), which is given by

$$VN(IM) = \sum_{i=1}^{N_b} CR_i \times E(LS_i \mid IM) \quad (1)$$

where VN (IM) is the building vulnerability, N_b is the number of building subassemblies, CR_i is the cost ratio of the i^{th} subassembly defined as the ratio of the repair or replacement cost for the entire i^{th} subassembly to the building value, E (LS_i | IM) is the expected loss ratio (LS_i) of the i^{th} subassembly (ratio of the damage repair or replacement cost for the i^{th} subassembly to the cost for repairing or replacing the entire subassembly) conditional on flood intensities, which can be evaluated based on physical damage ratios obtained from a damage assessment. Four building subassemblies (N_b = 4) were considered in the vulnerability assessment including wall siding, fenestrations, structural framing and building interior. The cost ratios for these subassemblies and the building components within each subassembly were estimated from Australian construction cost guide (Rawlinsons 2021). Note that this study only assesses building losses without considering contents losses.

If the building is not dry proofed, it is not unreasonable to assume that the water depth inside the building will eventually equal to the outside inundation depth for a flood event. The expected loss ratio of the building interior for a given inundation depth was derived based on the empirical and expert-elicited loss estimates in USACE (2006). The expected loss ratios for the remaining building subassemblies (wall siding, fenestration and structural framing) are related to the physical damage ratios of these subassemblies.

3.2. Physical damage of subassemblies

The building is subjected to lateral hydrostatic and hydrodynamic loads from floods that cause damage. Buoyancy force is not considered as an issue for this type of industrial building. Hydrostatic loads are present when there is a water depth difference inside and outside the

building. Hydrodynamic flood forces are due to the presence of flow velocities. The lateral hydrostatic and hydrodynamic loads were modelled based on the code-based load equations given by ASCE 7-16 (2017). The water depth difference during a flood event mainly depends on the outside flood rising rate and the water infiltration through small openings of the building envelope and breaches of the building envelope if wall siding and/or fenestration damage occurs. This study considers two bounding load cases for hydrostatic and hydrodynamic actions with respect to the water depth difference and the effect of building envelope damage.

Bounding load case I: The building has equalized water depths inside and outside, and hence only hydrodynamic load applies. This case may occur during slow-rise floods (generally riverine flooding) or when the building is wet-proofed.

Bounding load case II: For a certain period during a flood event, negligible water infiltrates inside, and therefore the maximum hydrostatic as well as hydrodynamic loads take effect if no damage occurs to the building envelope. However, when there are breaches of the building envelope, it is assumed that floodwater will quickly rise inside so that the hydrostatic loads are largely cancelled, and only hydrodynamic loads apply to the structural components. This case may occur during rapid-onset floods (e.g., flash flooding, high-intensity coastal flooding) or when the building is dry-proofed.

In this study, bounding load case I was assumed for riverine flood while both load cases were assumed possible for overland flow and coastal floods.

The physical damage assessment considers flood damage to the building envelope (wall siding and fenestration) and structural framing (portal frame and end wall frame). Wall siding panels fail if inward pressures from hydrostatic and hydrodynamic actions exceed the capacities of supporting girts. The girt failures were assessed by comparing flood loads with girt resistances to inward loads (statistics obtained from Qin et al. 2023). Fenestration (windows, entry doors and overhead roller doors) failures are caused by inward pressures from floods. The fenestration capacities were assumed to follow a normal distribution with statistics estimated from AS2047 (Standards Australia 2014), AS/NZS4505 (Standards Australia 2012) and FEMA (2014). The failure modes considered for a steel portal frame are bending failure of the column member and shear failure of the column base to concrete footing connection (i.e., hold down bolts). The flood demands on a portal column are the maximum bending moment on the column member and the maximum shear force at the column base. Nonlinear elastic structural analysis was used to obtain the flood demands on portal columns. In addition to internal forces induced by flood actions, the bending moment and shear force on a portal column due to dead load arising from the self-weight of building components are also considered in the structural analysis. The probabilistic capacity model and statistical information for column members and column base connections were built and estimated based on AS4100 (Standards Australia 2020), Pham et al. (1986) and Pham & Hogan (1986). The end wall frame damage is caused by failures of wind columns (member failure or column base connection failure), roof struts, roof and wall bracing. The probabilistic capacity models for these elements were built based on relevant standards (e.g., AS4100) and statistics from the literature (e.g., Pham et al. 1986; Pham 1987). The demands on these end wall frame components were obtained by elastic structural analysis.

The physical damage assessment suggests that building envelope (wall siding and fenestration) damage is more likely to occur than structural framing damage. Flood damage to structural subassemblies is mainly caused by hydrodynamic actions. The steel portal frame only fails under extreme flood loads (e.g., a flow velocity of 6 m/s with inundation depth over 4 m). End wall frame failures also occur with high hydrodynamic loads, though it is relatively more vulnerable than steel portal frame.

3.3. Vulnerability curves

Figure 5 shows the expected building loss ratios (vulnerability) considering the two bounding load cases and two orthogonal flow directions. The building interior loss as a function of inundation depth (not depend on flow velocity and direction) from the USACE study is also shown in the figures as a benchmark building loss (i.e., the building loss when no damage occurs to the building envelope and structural framing). The gap between a vulnerability curve and the interior loss curve represents the losses of the building envelope and structural framing. For the longitudinal flow direction perpendicular to the end wall, the higher the flow velocity, the higher the contribution of building envelope damage and end wall frame failure to the building vulnerability. For the bounding load case I, relatively low flow velocities only incur building interior losses due to floodwater inundation because the hydrodynamic loads are not significant enough to cause damage to other building subassemblies. For the bounding load case II, due to the presence of hydrostatic loads, building losses from damage to subassemblies other than building interior also exist for relatively low flow velocities. The sudden increases of vulnerability curves are due to the occurrence of end wall frame failure. For the transverse flow direction perpendicular to the long wall, the building vulnerability is less sensitive to flow velocities except for the flow velocity of 6 m/s as portal frame failure start to occur at this velocity, which cause this sudden increase of the building vulnerability. The combined repair/replacement cost of wall siding and fenestration is much less than other building subassemblies (e.g., building interior, structural framing). This explains that, if no frame failure occurs, the differences between building vulnerabilities corresponding to different flow velocities (the gap between a vulnerability curve and the interior loss curve) are not prominent.

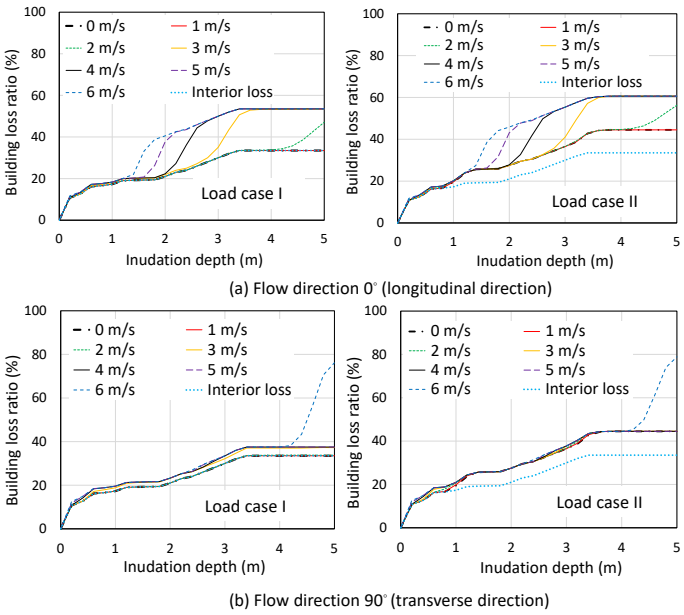

Figure 5: Expected building loss ratios (vulnerability) for various inundation depths and flow velocities considering two bounding load cases and two orthogonal flow directions.

4. LOSS ESTIMATION

The building losses were estimated for selected industrial buildings within the industrial area shown in Fig. 1 under different types of floods with a 100-year ARI and 500-year ARI for current and future climates. The selected industrial buildings are shown in Fig. 6, and they have similar geometries, structural configurations and construction materials with the prototype industrial building in Fig. 4. The replacement values were assumed the same for all selected buildings, though this may change once detailed exposure data and building surveys are available.

Flood velocities were not revealed by previous flood studies described in Section 2. This study considers two possible velocities (i.e., 0 m/s and 1 m/s) for riverine flood, and three possible velocities (i.e., 1 m/s, 3 m/s and 5 m/s) for overland flow and coastal floods. For simplicity, either a longitudinal or a transverse flow direction was assigned to each building depending on its orientation. The aggregated building losses were evaluated based on developed vulnerability model

and the flood intensities (inundation depths and flow velocities) at individual building levels.

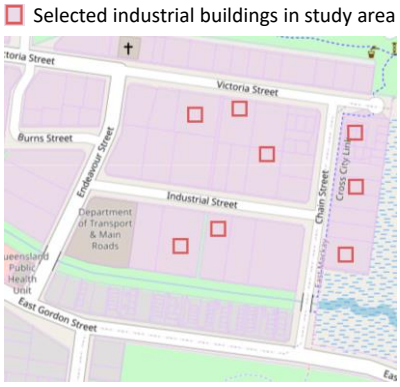

Figure 6: Selected industrial buildings for loss estimation.

The analyses suggest that all the selected industrial buildings have sufficient floor height to avoid being inundated (i.e., no building losses) by the three types of floods with a 100-year ARI under the current climate. Considering the climate change impacts on 100-year ARI floods, some buildings could be inundated by up to 0.8 m water depth for riverine flood and up to 0.6 m water depth for coastal flood, whereas still no inundation for overland flow (pluvial) flood, hence no building losses for this type of flood even with the adverse climate change impacts. It was found that, for 100-year floods, the mean aggregated building loss ratios by 2100 with climate change impacts increase from nil (no building losses under the current climate) to about 5.1% for coastal flood, and from nil to 8.4% for riverine flood. As the inundation depths are relatively low, the effects of flow velocities and load cases on aggregated building losses are marginal.

For the three types of floods with a 500-year ARI under the current climate, the selected industrial buildings could be inundated by up to 0.9 m water depth for riverine flood, up to 0.7 m water depth for coastal flood and still no inundation for overland flow flood. For the future climate by 2100, the selected industrial buildings could be inundated by up to 1.6 m water depth for riverine flood, up to 1.8 m water depth for coastal flood and up to 0.2 m water depth for overland flow flood. The aggregated building loss is only increased marginally for overland flow floods with climate change impacts. Figure 7 shows the mean aggregated building losses considering different load cases and flow velocities for 500-year riverine and coastal floods under the current and future climates. The figure suggests that, for the current case study with the highest inundation depth well under 2 m, the effects of load cases and flow velocities on the aggregated building losses are not significant for both riverine and coastal floods under both climate scenarios. This may change if more significant flood inundation are predicted. The climate change impacts increase building losses by about 47.2% for riverine flood with a 500-year ARI, and by about 176.6% on average for coastal flood with a 500-year ARI.

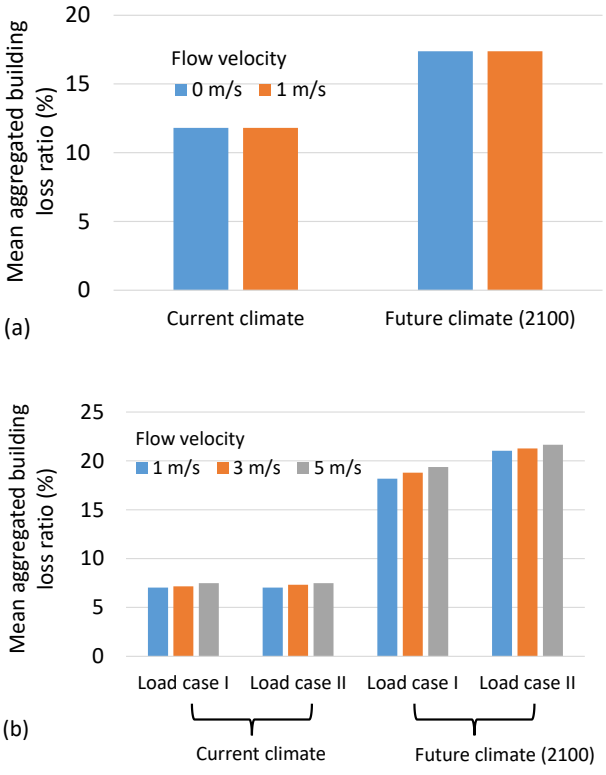

Figure 7: Aggregated building loss ratios for 500-year floods under the current and future climates, (a) riverine flood, (b) coastal flood.

5. CONCLUSIONS

This case study estimated building losses for an industrial area exposed to flood hazards and climate change risks in the City of Mackay, Australia. The flood inundation risks for the study area under current and future climates were obtained from data produced by previous flood studies. Various flood types including riverine (fluvial), overland flow (pluvial) and coastal (storm tide) floods were considered for industrial buildings in the study area. A high-fidelity physics-based vulnerability model was developed for a prototype steel portal frame industrial building considering major damage mechanisms for building components under flood-induced hydrostatic and hydrodynamic loads. Aggregated building losses were then evaluated based on the vulnerability model and the predicted extreme flood inundation at individual building levels for different ARIs considering the climate change impacts. It was found that the climate change impacts on building losses for 100-year floods are marginal. However, for 500-year floods in year 2100, the aggregated building losses could potentially increase by about 47% for riverine flood and about 176% for coastal flood, whereas the climate change impacts on building losses due to overland flow flood are negligible. Different types of floods were assessed separately in this study, but future research may consider the effects of compound floods. Less conservative emission scenarios for future climate are also needed to be considered.

6. REFERENCES

ASCE (2017). *ASCE/SEI 7-16 Minimum design loads for buildings and other structures*, American Society of Civil Engineer, Reston, VA, USA.

Ball J, Babister M, Nathan R, Weeks W, Weinmann E, Retallick M, Testoni I, (2019). *Australian Rainfall and Runoff: A Guide to Flood Estimation*, Commonwealth of Australia (Geoscience Australia), Canberra, Australia.

BMT WBM (2013). *Mackay Region Storm Tide Study*, Report prepared for Mackay Regional Council by BMT WBM Pty Ltd, Brisbane, Australia.

FEMA (2014). *Hazus Hurricane Model Technical Manual*. Federal Emergency Management Agency, Mitigation Division, Washington DC, USA.

Pham, L. (1987). "Safety index analyses of tension members". *Civil Engineering Transactions, Institution of Engineers Australia*, CE29(2), 128-130.

Pham, L., & Hogan, T. J. (1986). "Calibration of the proposed limit states design rules for bolted connections". *Civil Engineering Transactions, Institution of Engineers Australia*, CE28(4), 292-297.

Pham, L., Bridge, R. Q., & Bradford, M. A. (1986). "Calibration of the proposed limit states design rules for steel beams and columns". *Civil Engineering Transactions, Institution of Engineers Australia*, CE28(3): 268-274.

Qin, H., Mason, M., & Stewart, M. G. (2023). "Fragility assessment for new and deteriorated portal framed industrial buildings subjected to tropical cyclone winds". *Structural Safety*, 100, 102287.

QLD GOV (2011). *Queensland Coastal Plan*. The Queensland Department of Environment and Resource Management, Queensland, Australia.

Rawlinsons (2021). *Rawlinsons Construction Cost Guide 2021*, Rawlinsons Publishing, Perth, Australia.

Standards Australia (2012). *Garage doors and other large access doors*, AS/NZS4505, Standards Australia.

Standards Australia (2014). *Windows and external glazed doors in buildings*, AS2047, Standards Australia.

Standards Australia (2020). *Steel structures*, AS4100, Standards Australia.

USACE (2006). *Depth-Damage Relationships for Structures, Contents, and Vehicles and Content-to-Structure Value Ratios (CSVR) in Support of the Donaldsonville to the Gulf, Louisiana, Feasibility Study*, US Army Corps of Engineers, LA, USA.

WRM (2021a). *Pioneer River Flood Study*, Report prepared for Mackay Regional Council by WRM Water & Environment, Brisbane, Australia.

WRM (2021b). *Mackay City Flood Study*, Report prepared for Mackay Regional Council by WRM Water & Environment, Brisbane, Australia.